Development of new hybrid ultrafiltration membranes by entanglement of macromolecular PPSU-SO$_3$H chains: Preparation, morphologies, mechanical strength, and fouling resistant properties

Thanigaivelan Arumugham, Noel Jacob Kaleekkal, Mohan Doraiswamy
Department of Chemical Engineering, Membrane Laboratory, Anna University, Chennai, Tamil Nadu 600025, India
Correspondence to: M. Doraiswamy (E-mail: mohantarun@gmail.com)

ABSTRACT: The present work focuses on the preparation of Polyphenylsulfone (PPSU) membranes with enhanced antifouling surfaces through an incorporation of sulfonated Polyphenylsulfone (PPSU-SO$_3$H), which acts as both, surface modifying agent and macromolecular additive. Initially, Sulfonated polyphenylsulfone (PPSU-SO$_3$H) was synthesized by using chlosulfonic acid via bulk modification method. The degree of sulfonation (DS, %) of PPSU-SO$_3$H was calculated by using NMR (nuclear magnetic resonance). The phase inversion technique was used to prepare all asymmetric membranes by allowing the PPSU-SO$_3$H (different wt %) to entangle with the PPSU membrane matrix. All prepared membranes were characterized by using scanning electron microscope (SEM), X-ray diffraction analysis (XRD), contact angle analysis (CA), mechanical strength analysis, molecular weight cut off (MWCO), porosity (%), mean pore size, and BSA adsorption studies. The performance efficiency of the membranes was evaluated by using BSA protein as a model foulant in terms of permeability, rejection (SR %), R_m (hydraulic resistance), R_c (cake layer resistance), R_p (pore plugging resistance), R_r (reversible fouling), R_{ir} (irreversible fouling), and FRR (flux recovery ratio). © 2015 Wiley Periodicals, Inc. J. Appl. Polym. Sci. **2015**, *132*, 41986.

INTRODUCTION

Currently, ultrafiltration (UF) membranes are being used in various fields such as biotechnology, food industries, pharmaceutical industries, chemical industries, water processing etc.[1] UF membranes are particularly involved in the processes of protein purification and concentration during the development new drug discoveries with high purity.[2] In general, most of the polymers have been used in preparation of UF membranes such as PA, PI, PVDF, PAN, PES, PEI, and PPSU etc.[3] Among them, sulfone group based polymers, like Polyphenylsulfone (PPSU) is a better candidate, because of its amorphous nature, high thermal stability, high mechanical strength, good chemical resistance (pH at 1–13) and chlorine tolerance.[4,5] However, due to the hydrophobic nature of PPSU membrane, it is easily prone to severe fouling during water treatment. The major types of fouling can be classified as organic fouling, inorganic fouling, biofouling, etc.[6] Furthermore, these can be categorized as reversible fouling and irreversible fouling. Among them, an irreversible fouling or pore plugging affects the membrane properties like permeation rate and selectivity. This can be solved by various methods such as pretreatment of feed, optimization of operation condition, chemical cleaning etc. However, these meth-

ods increase the operation cost of the membranes and affect the life time of the membranes.[7] To address this problem, various modification methods have been employed to make the hydrophilic surfaces, which in turn stimulates lower attachment by foulants. Recently, there are various methods have been reported on preparation of hydrophilic membranes such as coating, grafting, bulk modification, plasma treatment, nanocomposites etc.[8] Among them, bulk modification like sulfonation receives attention by researchers, due to simple, rapid modification method, and induces more hydrophilic properties of polymers.[9] However, using 100% PPSU-SO$_3$H membrane does not show sufficient mechanical strength, due to the high swelling nature of PPSU-SO$_3$H polymer and degradation of polymeric chain length.[10] In the recent years, a lot of research is being done on sulfonated polymers in the field of fuel cell, batteries etc.[11–13] There are few reports available on preparation and studies on PPSU-SO$_3$H in UF applications. To address this issue, preparation of fouling resistant PPSU-SO$_3$H membranes with sufficient mechanical strength has been taken up as a challenge in the present work.

In the present study, sulfonation reaction was carried out by one step reaction using chloro sulfonic acid as a sulfonation
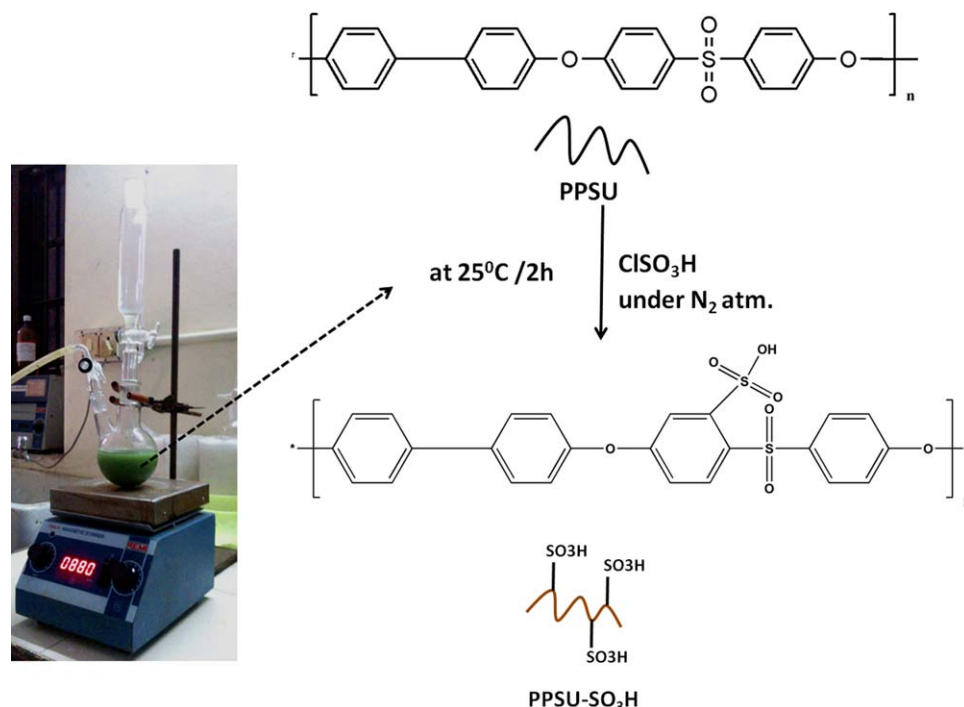
Figure 1. Sulfonation reaction scheme of poyphenylsulfone(PPSU-SO$_3$H). [Color figure can be viewed in the online issue, which is available at wileyonlinelibrary.com.]

agent and confirmed through NMR spectra. The different wt % of sulfonated PPSU chains (PPSU-SO$_3$H) were allowed to entangle with PPSU chains by using phase inversion method, which is suitable for preparation of asymmetric membranes. An influence of different concentrations of PPSU-SO$_3$H entanglement was investigated in detail by using SEM, XRD, mechanical strength analysis, contact angle, permeation studies (flux). In addition, fouling resistant properties of all membranes were evaluated using BSA (bovine serum albumin) as model foulant in terms R_m (hydraulic resistance), R_c (cake layer resistance), R_p (pore plugging resistance), R_r (reversible fouling), R_{ir} (irreversible fouling), and FRR (flux recovery ratio).

MATERIALS AND METHODS

PPSU (M_w: 53,000–59,000 g/mol), chlorosulfonic acid (99%), sodium azide ($\geq$9.5%), polyethylene glycol (PEG 200): all the chemicals were received from Sigma-Aldrich, India. N-methyl-2-pyrolidone, extra pure (NMP, from Sisco Research, India), n-Hexane (synthesis) from Merk Specialties, India. Sodium laryl sulfate (pure), (Sisco Research, India). Dextran (M_w: 10,000 Da, 20,000 Da, 40,000 Da, and 70,000 Da) from HiMedia Laboratories, India. Ethyl alcohol (AR), 99% (v/v) min was received from Hayman Speciality products, UK. Pure distilled water was used to prepare the coagulation bath.

Synthesis of Sulfonated Polyphenylsulfone (PPSU-SO$_3$H)
The sulfonation reaction was carried out as mentioned in previous literature.[14] The complete reaction scheme is given in the Figure 1. The resultant sulfonated polyphenylsulfone (PPSU-SO$_3$H) product was confirmed through H^1-NMR spectra

(Bruker AMX 400FT) and degree of sulfonation was calculated from corresponding NMR peaks.

Preparation of Membranes
The simple wet phase inversion method was used to prepare all PPSU-SO$_3$H entangled PPSU UF membranes which were reported in the literature.[15] The different compositions of polymeric casting solution were prepared as mentioned in Table I. The resulting casting solution was stirred for 12 h at room temperature to become a homogeneous solution. After that, the viscous polymeric casting solution was kept for 4 h to remove the air bubbles. The homogeneous casting solutions were casted on the glass plate using Doctor's blade under controlled environment such as relative humidity (25 ± 2%) and temperature (40°C).

Meanwhile, the coagulation bath was prepared with particular compositions such as 2% (v/v) of NMP (solvent), 0.2 wt % of SLS (surfactant) in 2 L of distilled water at 14 ± 2°C.

After casting the polymeric solution, the glass plate was immersed into the coagulation bath to initiate phase inversion

Table I. Composition of the PPSU-SO$_3$H/PPSU Membranes

Membrane	PPSU (wt %)	PPSU-SO$_3$H (wt %)	NMP (wt %)
b	100	–	84
S1	95	05	84
S2	90	10	84
S3	85	15	84
S4	75	25	84

Total PPSU polymer concentration at 16 wt %.

process. The resultant membranes were peeled off, washed with distilled water to remove residual solvents and surfactant and stored in the distilled water containing sodium azide (100 mg/L) to avoid unwanted bacterial growth on the surface of the membranes. All the membranes were prepared with uniform thickness (0.22 ± 0.02 mm) and checked using digimatic caliber with a precision of 0.001 mm.

CHARACTERIZATION OF MEMBRANES:

Analysis of Membrane Morphology

The prepared membranes were characterized using scanning electron microscope (SEM, Cam Scan MV 2300). Initially, the membranes were cut into desired shape after being freeze dried in liquid nitrogen for 60–90 S. The non conducting membranes were gold sputtered to make electrical conductivity on membrane surface. The cross sectional and surface images were captured under high vacuum (10 kV) condition.[16]

X-ray Diffraction (XRD) Analysis

The polymeric chain packing efficiency of the membranes was characterized using Wide angle X-ray diffraction pattern (Bruker AXS D8 Advance X-ray diffractometer).[17] The diffraction patterns were recorded within the range 5°–70° using CuKα radiation ($\lambda = 1.54$ Å).

Mechanical Strength Analysis of Membranes

The mechanical strength of all the prepared membranes was measured under ASTM method D882, using the instrument (H1KT UTM, Tinius Olsen, PA). All the membranes were cut in to the specific dimension of 1 × 5 inches. The excess of water in the membranes was removed and the ambient conditions were maintained (25°C, relative humidity 60%). Three measurements were taken for each membrane and average values were reported.[18]

Contact Angle of the Membranes

All prepared membranes were cut into (2 × 2 cm^2) size, washed completely in distilled water, and the membrane surface was mopped with tissue paper. Then, contact angle of all membranes was measured using GBX instrument, Germany at 25°C as reported in the Ref. [19. A 2 µL of milli-Q water was placed on the membrane to form a sessile drop, angle of the sessile drop was measured within 5 s, at five different locations for each membrane and average value of angle was reported.

Pure Water Flux (PWF)

After compaction at 414 kPa, pure water permeation was measured for all membranes prepared for every one hour in the UF cell (Model 8400, Amicon, USA) with an internal diameter of 76 mm at specific operating pressure (345 kPa) at 25°C. The amount of pure water flux (J_{w_1}) was calculated using eq. (1). For each membrane, pure water flux experiment (J_{w_1}) was conducted in three different areas and average values were reported for accuracy.

$$J_{w_1} = \frac{Q}{A(\Delta t)} \qquad (1)$$

Molecular Weight Cut-Off (MWCO) Analysis

The experiment was performed with UF cell (Model 8400, Amicon, USA), dead end filtration setup at 345 kPa using

Dextran (0.2 g/L) solution with different molecular weights (20, 40, and 70 kDa) to determine the pore size of the membranes.[20] Total organic carbon analyzer (Shimadzu, TOC-V CPH) was used to analyze the concentration of feed and permeate of the corresponding membranes. The MWCO of membrane can be defined the size of low molecular weight solute, which shows the highest rejection percentage of 90%.

The rejection of membranes was calculated using eq. (2),

$$SR(\%) = \left[1 - \left(\frac{C_p}{C_f}\right)\right] \times 100 \qquad (2)$$

C_p is the concentration of permeate (g/L); C_f is the concentration of feed (g/L).

Analysis of Porosity and Mean Pore Size (nm) of the Membranes

Porosity (ε, %) of all prepared membranes was calculated by gravimetric method.[21,22] It can be defined as the ratio between presence of water content in the pores and volume of the pores of the membrane. The given eq. (3) was used to determine the porosity of the membranes and the average value of five experiments was reported for each membrane:

$$\varepsilon(\%) = \frac{W_0 - W_1}{\rho A h} \times 100 \qquad (3)$$

where W_0 is the wet weight of the membrane; W_1 is the dry weight of the membrane; ρ is the density of water (0.998 g cm^{-3}); A is the effective membrane area (m^2); h is the membrane thickness (cm).

Guerout–Elford–Ferry eq. (4) was used to calculate the mean pore size (r_m) of all prepared membranes based on the results of pure water flux (J_{w_1}) and porosity value.[23]

$$r_m = \sqrt{\frac{(2.9 - 1.75\varepsilon)8\eta h Q}{\varepsilon \times A \times \Delta P}} \qquad (4)$$

where η is the water viscosity (8.9 × 10^{-4} Pa s), Q is the quantity of permeate of pure water flux per unit time (m^3 S^{-1}), ΔP is the operating pressure (345 kPa), h is the membrane thickness (m), and ε is the porosity of the membranes.

Analysis of BSA Adsorption

The adsorption experiment was carried out as reported in the Ref. [24. All the membranes were analyzed using BSA (bovine serum albumin) protein molecules to evaluate the adsorption capacity of the membrane surface. At first, 1 mg/mL of BSA (pH = 7) was prepared to conduct the adsorption studies. Then, all the membranes were cut to have similar area of 19.6 cm^2. Each membrane was placed to contact with 10 mL of BSA protein solution and kept on the mechanical shaker for 24 h at 25°C. UV–Visible spectrometer (Bio-chrome) was used to determine the concentrations of BSA proteins at 280 nm. Finally, the amount of adsorbed proteins was calculated using eq. (5).

$$\textit{Amount of Absorbed Protein}(\%) = \left[\frac{C_0 - (C + C_w)}{A}\right] \times 100 \qquad (5)$$

Here, C_0 is the initial concentration of BSA protein solution before adsorption experiment; C si the concentration of protein in solution after adsorption experiment; C_w is the concentration
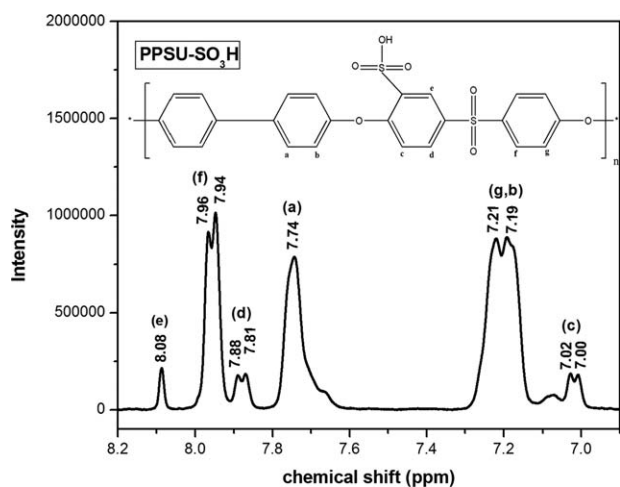
Figure 2. NMR analysis of sulfonated polyphenylsulfone (PPSU-SO$_3$H).

of protein after washing in PBS solution; A: effective membrane area (cm^2).

Analysis of BSA Rejection
Before the experiment, the BSA (1 g) was dissolved in 1000 mL of PBS (pH = 7). To evaluate the filtration ability with rejection, the prepared membranes were subjected to filtration of BSA protein at constant pressure of 345 kPa for 2 h using dead end ultra filter cell. During the experiment, concentration polarization was minimized significantly by stirring the protein solution using magnetic stirrer at 300 rpm. The resultant rate of permeate was calculated using the following eq. (6):

$$J_P = \frac{Q}{A(\Delta t)} \qquad (6)$$

Q is the volume of permeate (L), A is the area of membrane (m^2), Δt is the permeate time (h).

At the same time, collected permeate was analyzed using UV spectrophotometer at wavelength 280 nm. The BSA rejection performance was analyzed using eq. (7), as reported in the Ref. [25.

$$R(\%) = \left[1 - \left(\frac{C_p}{C_f}\right)\right] \times 100 \qquad (7)$$

C_p is the concentration of permeate; C_f is the concentration of feed.

Analysis of Antifouling Properties of Membranes:
After filtration of BSA protein solution, all the membranes were cleaned using distilled water for 15 min. The cleaned membranes were subjected to pure water flux (J_{w_2}) for 5 h at a pressure of 345 kPa. Permeate of the membranes was measured for every 1 h.

The fouling resistant properties of the membranes were calculated[26,27] by using following eqs. (8–10).

$$\text{Reversible fouling } R_r = \frac{J_{w_2} - J_{w_p}}{J_{w_1}} \times 100 \qquad (8)$$

$$\text{Irreversible fouling } R_{ir} = \frac{J_{w_1} - J_{w_2}}{J_{w_1}} \times 100 \qquad (9)$$

$$\text{Flux recovery ratio FRR}(\%) = \frac{J_{w_2}}{J_{w_1}} \times 100 \qquad (10)$$

J_{w_1} is the pure water flux (lm^{2}h^{-1}): J_{w_2} is the pure water flux after cleaning the membranes (lm^{2}h^{-1}); J_{w_p} is protein flux (lm^{2}h^{-1}).

The filtration process across the membrane contributes the resistance against flow, the resistance in series model is used to evaluate the characteristics membrane surface during filtration to determine the extent of fouling.[28]

$$J = \frac{\Delta p}{\mu R_t} \qquad (11)$$

$$R_t = R_m + R_c + R_p \qquad (12)$$

where R_m is the hydraulic resistance (m^{-1}), R_c is the resistance due to cake layer formation on the membrane surface (m^{-1}), R_p is the resistance due to the solute plugging in to the pore wall in filtration (m^{-1}). Each resistance can be calculated using the following equations,

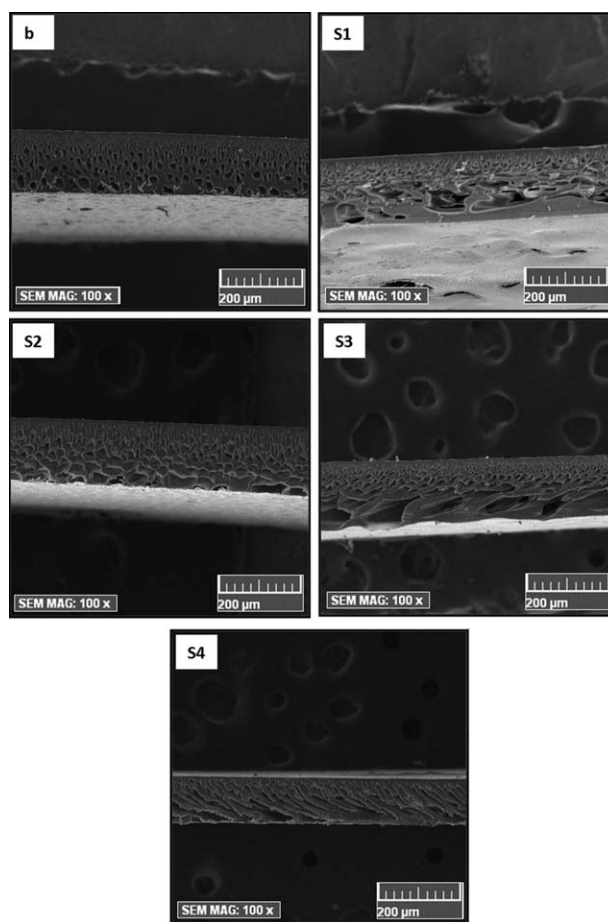$$R_m = \frac{\Delta P}{\mu J W_1} \qquad (13)$$

Figure 3. (a) Cross-sectional morphological images of PPSU-SO$_3$H-PPSU membranes. (b) Top surface morphological images of PPSU-SO$_3$H -PPSU membranes.
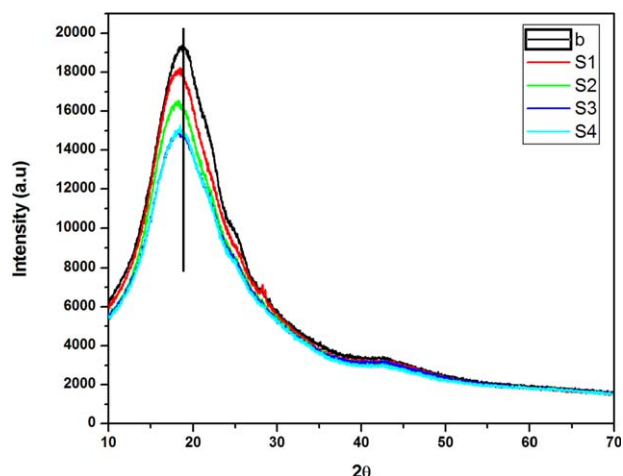
Figure 4. X-ray diffraction analysis of PPSU-SO₃H-PPSU membranes. [Color figure can be viewed in the online issue, which is available at wileyonlinelibrary.com.]

$$R_p + R_c = \frac{\Delta P}{\mu J W_p} - R_m \qquad (14)$$

$$R_p = \frac{\Delta P}{\mu J W_2} - R_m \qquad (15)$$

where J_{w_1} is the pure water flux of the membranes, J_{w_2} is the pure water flux after cleaning the membranes (lm^2h^{-1}); J_{w_p} is protein flux (lm^2h^{-1}), ΔP is the operating pressure during membrane filtration, μ is the viscosity of the permeate solution.

RESULTS AND DISCUSSION:

Characterization of Sulfonated Polyphenylsulfone (PPSU-SO₃H) and Membrane Preparation

The H^1-NMR spectrum of sulfonated PPSU is shown in Figure 2. All the characteristic proton signals appeared in the chemical shift range of 7–8.5 ppm. The major singlet peak for corresponding proton (H_e) is observed at 8.08 ppm, which confirms the presence of sulfonic acid on PPSU. Furthermore, the degree of sulfonation (DS %) was calculated based on corresponding proton (H_e) of PPSU-SO₃H, which was reported in the earlier Ref. [29, the DS (%) value was 31.9%. During membrane preparation, Adding of 5–25 wt % of PPSU-SO₃H in the casting solution provides sufficient entanglement with PPSU chains to produce a stable homogeneous membrane surface. Further addition of 35wt % of PPSU-SO₃H leads to inhomogeneous membrane surface. This can be due to insufficient entanglement with PPSU chain, which leads to considerable leaching out of PPSU-SO₃H.[8]

Morphology of the Membranes

The Figure 3(a,b) shows the cross-sectional and top surface morphologies of the modified and pure PPSU membranes.

The pure PPSU membrane (b) shows a macro void structure with a dense skin layer as shown in the Figure 3(b). During the membrane formation process, the dense skin layer of PPSU restricts the passage of nonsolvent into the polymer poor phase. This induces the growth of single pore nuclei into a macro porous structure.[30] In case of modified membranes [Figures 3(a,b), S1–S4, Supporting Information], the sulfonic acid polar moiety on PPSU-SO₃H increases the demixing time between nonsolvent and solvent (NMP). This is due to the strong H-bond interaction between acid group (—OH) and water molecules, which increases the more penetration time for nonsolvent (water). This longer penetration time facilitates the growth of number of small pore nuclei, which can coalescence with each other to interconnect the top and bottom surface of membrane. As a result, specifically, the 15–25 wt % of PPSU-SO₃H entangled PPSU membranes, exhibit a highly porous morphology [shown in Figures 3(a,b), S3, S4, Supporting Information].

Analysis of X-ray Diffraction Pattern (XRD) of Membranes

The XRD pattern of all membranes is shown in the Figure 4, and the calculated inter planar distance (nm) is given in the Table II. In general, XRD is a technique which is commonly used to predict the properties of polymers such as crystalline, semi crystalline, and amorphous. Here, the PPSU membrane (b) gives a broad intense peak at 18.7°. The modified membranes S1, S2, S3, and S4 were observed to have 2θ of 18.47, 18.39, 18.37, and 18.30, respectively. This reliable 2θ shift to lower angle indicates that the addition of PPSU-SO₃H polymer makes incompatible physical interaction (or) forces such as weak van der waals force between PPSU-SO₃H and PPSU polymeric chain, which could enhance the inter plane distance (Table I). The reduction of peak intensity was a result of irregular chain packing, during membrane formation. In general, the membrane, which has a higher planar distance, may increase the permeation rate of pure water molecules. Particularly, addition of 25 wt % of PPSU-SO₃H, improves the inter plane distance value to 0.484 nm (S4) from 0.473 nm (a1). Similar result was observed by Rachipudi et al.,[31] where pure PVA shows high intense crystalline XRD peak, the peak intensity was decreased significantly by crosslinking with sulfophthalic acid (SPTA), which acts as an amorphous domain.

Mechanical Strength Analysis of Membranes

The Figure 5 displays the tensile strength of all prepared membranes. The pure PPSU membrane (b) has a tensile strength

Table II. Porosity, MWCO, Mean Pore Size, d-Spacing of the Membranes of Membranes

Membrane	Porosity (%)	MWCO (kDa)	Mean pore size (μm)	d-spacing (nm)
b	24.61 (±0.52)	40	0.0152 (±0.015)	0.473 (±0.002)
S1	32.45 (±1.21)	40	0.0156 (±0.013)	0.479 (±0.001)
S2	36.13 (±1.12)	40	0.0159 (±0.012)	0.481 (±0.002)
S3	39.97 (±1.46)	40	0.0167 (±0.014)	0.483 (±0.001)
S4	48.09 (±2.02)	70	0.0180 (±0.017)	0.484 (±0.001)

Table III. Permeation Properties, BSA Rejection and Fouling Analysis

Membrane	Flux (Lm^{-2}h^{-1})			R_r (%)	R_{ir} (%)	FRR (%)	Rejection (%) BSA
	J_{w_1}	J_p	J_{w_2}				
b	116 (±1.15)	26.3 (±0.28)	53.6 (±1.52)	23.5 (±1.32)	54.0 (±1.01)	45.9 (±0.11)	97.6 (±0.36)
S1	148 (±2.88)	29.0 (±1.01)	95.6 (±1.15)	44.9 (±1.15)	35.4 (±1.10)	64.5 (±0.23)	97.5 (±0.54)
S2	165 (±1.52)	35.3 (±2.08)	112.3 (±2.10)	46.5 (±1.15)	32.0 (±0.75)	67.9 (±0.17)	97.4 (±0.23)
S3	183 (±3.60)	38.0 (±1.00)	132.6 (±1.56)	51.7 (±1.15)	27.4 (±2.03)	72.5 (±0.32)	96.7 (±0.42)
S4	218 (±1.52)	44.6 (±0.55)	174 (±2.02)	59.2 (±1.15)	20.3 (±0.90)	79.6 (±0.62)	85.4 (±0.63)

J_{w_1} = pure water flux (L m^{-2} h^{-1}); J_p = protein solution flux (L m^{-2} h^{-1}); J_{w_2} = pure water flux or permeation rate, after cleaning the membranes (L m^{-2} h^{-1}); R_r = reversible fouling (%); R_{ir} = irreversible fouling (%); FRR = flux recovery ratio (%).

value of 3.0 (±0.15) Mpa. In general, an increase in tensile strength value indicates a higher stacking of polymeric chains. When incorporating PPSU-SO$_3$H, the tensile strength values of the membranes decrease (shown in Figure 5), which is due to the influence of PPSU-SO$_3$H on polymeric chain stacking of PPSU. However, the modified membranes (S1–S3) show the almost similar tensile strength values of 2.6 (±0.1) Mpa, 2.55(±0.13) Mpa, and 2.3(±0.14) Mpa, respectively. Among the modified membranes, addition of 25 wt % (membrane S4), shows a very low tensile strength value 1.7 (±0.1) Mpa. This may due to the incompatibility of polymeric chains, which causes more steric irregularity in arrangement of polymeric chains.[32,33] The results of XRD pattern also suggest the same trend, which is due to the polymeric chain packing arrangement (shown in Figure 4).

Hydrophilicity and Pure Water Flux of the Membranes

Figure 6 shows the contact angle (CA) images of all membranes. In general, lower contact angle value represents the hydrophilic character and vice versa. Among the membranes, the pure PPSU (b) shows high contact angle value of 72°, which indicates the more hydrophobic characteristic membrane surface. After entanglement of PPSU-SO$_3$H polymeric chain (different wt %), the contact value shows significant decreases up to 54.9°. This may be due to the existence of H-bond interaction between water molecule and polar sulfonic acid group.[34] Further, the pure water flux experiment was conducted for all membranes to determine the rate of permeation for water molecules. All modified membrane show the better flux profile than pure PPSU membranes, shown in Figure 7. The pure PPSU has given lower flux rate of 116 (±1.15). When incorporating 15% and 25% of PPSU-SO$_3$H, the flux was increased up to 183 (±3.60) and 218 (±1.52), respectively. This can be due to the presence of hydrophilic PPSU-SO$_3$H polymeric chain with PPSU chain. Thus, this increases the free volume between polymeric chains, which allows more number of water molecules across the membrane. As a result, the PPSU-SO$_3$H polymeric chain entangled membranes showed better improvement in hydrophilic character to increase the pure water flux. These observations are similar to those reported by Arthanareeswaran et al.[35]

Analysis of Membrane Porosity, Pore Size, and MWCO

The porosity of all membranes was evaluated and results are given in Table II. In general, porosity can be defined as number of pores per unit volume of the membrane. When incorporating

PPSU-SO$_3$H chain, the hydrophilic sulfonic acid group allows the more number of water molecules to form more pore nuclei and this enhances the surface porosity of modified membranes (S1–S4). However, in the case of Pure PPSU (b), the hydrophobic character restricts the passage nonsolvent (water), during solvent-nonsolvent exchange process, which may be due to high surface tension of PPSU. As a result, the pure PPSU (b) shows a lower porosity value of 24.61(±0.52) than that of modified membranes (S1–S4). Among them, the membranes (S3–S4) show reliable high porosity values of 39.97(±1.46) and 48.09(±2.02), respectively. Also, pore size of the membrane is one of the major factors to evaluate the membrane performance in terms of rejection and permeation. Adding PPSU-SO$_3$H shows slight increases in mean pore size and gives same MWCO for all modified membranes, except membrane S4 (shown in the Table II). This is due to the addition of 25 wt % of PPSU-SO$_3$H which causes the incompatibility between polymeric chains, which can in turn, increase the pore size of the membrane.[36]

BSA Adsorption Analysis

The protein adsorption study revealed the effect of sulfonic acid group on BSA protein molecules. In general, a hydrophilic material induces weak interaction with hydrophobic (protein) molecules. As shown in Figure 8, The protein adsorption of Pure PPSU (b) is 11.9 ± (1.1). After modification with PPSU-SO$_3$H (different wt %), the amount of protein adsorption
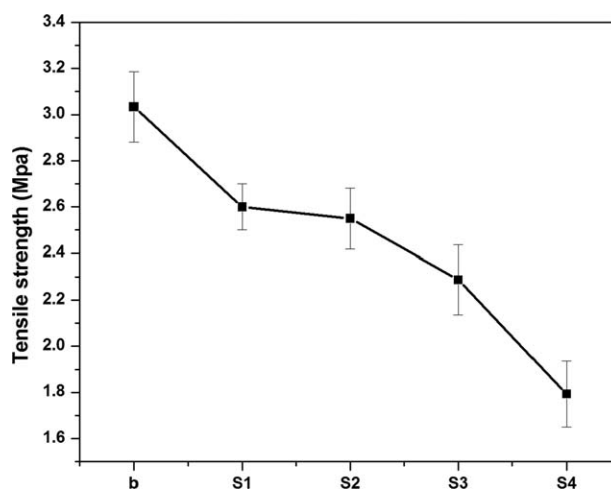
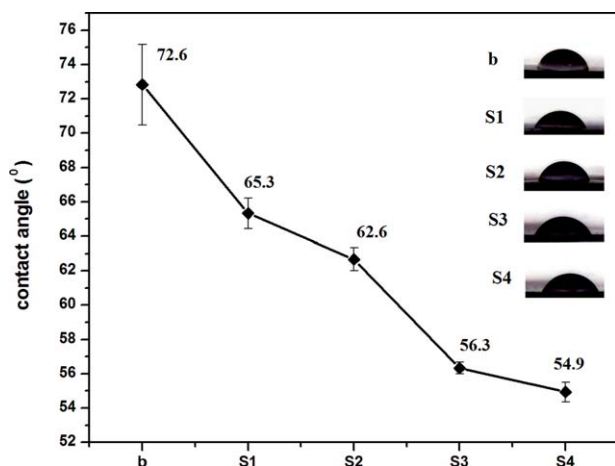**Figure 5.** Mechanical strength analysis of PPSU-SO$_3$H-PPSU membranes.

Figure 6. Contact angle analysis of PPSU-SO$_3$H-PPSU membranes. [Color figure can be viewed in the online issue, which is available at wileyonline-library.com.]

Figure 8. BSA adsorption analysis of PPSU-SO$_3$H -PPSU membranes.

decreased to 5.5 ± (0.15), 4.6 ± (0.19), 4.6 ± (0.30), and 3.8 ± (0.24) for membranes b, S1, S2, S3, and S4, respectively. This can be due to more entanglement of PPSU-SO$_3$H chains into the PPSU membrane matrix, which may cause antiprotein attachment on wet surface by increasing number of fraction of water molecules.[37] As reported in the previous Ref. 38, BSA shows isoelectric point at pH = 4. At pH = 7, protein molecules get negative potential in PBS. As a result, negative charged sul-fonic acid modified membranes prevent the strong protein adsorption, due to increase of electrostatic repulsive force against negative charged BSA protein molecules.

Antifouling Analysis

BSA (bovine serum albumin) protein filtration was carried out by prepared membranes to evaluate the fouling resistant surface characteristics. The protein permeation results of all membranes are shown in the (Figure 7). Among them, PPSU membrane (b) showed lower protein flux profile than was observed for pure
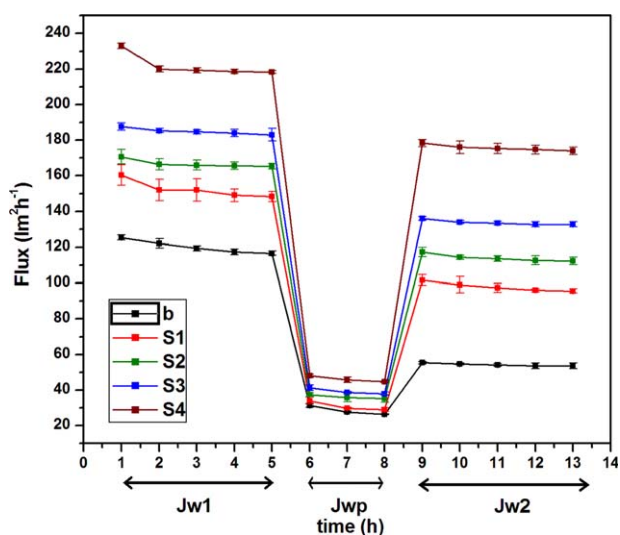
PPSU membrane (b), which shows steady state flux (J_p) of 26.3 (±0.28) lm^{-2}h^{-1}. This is due to the hydrophobic nature of PPSU membrane surface, which drives the proteins molecules to adhere or accumulate on the membrane surface. When incor-porating the PPSU-SO$_3$H, the flux was improved significantly, because of the presence of hydrophilic sulfonic acid group on the PPSU membrane surface and pores. In addition, to evaluate the fouling resistant properties, R_m (hydraulic resistance), R_c (Cake layer resistance), and R_p (pore plugging resistance) were calculated for all membranes and values are displayed in the (Figure 9 and Table IV). The modified membranes S1, S2, S3, and S4 has a lower R_m value of 0.94(±0.07), 0.84(±0.02), 0.76(±0.08), and 0.64(±0.17), respectively, which indicates that highly hydrophilic membrane surface provides lower resistance for water molecules to pass across the membrane.[39] Furthermore, R_c (Cake layer resistance) and R_p (pore plugging resistance) were analyzed to understand the interaction between BSA protein and membrane surfaces. Addition of 15–25 wt % of PPSU-SO$_3$H increases the water cluster on the PPSU mem-brane surface. The wet membrane surface tends to lower the

Figure 7. Permeation results of PPSU-SO$_3$H -PPSU membranes. [Color figure can be viewed in the online issue, which is available at wileyonline-library.com.]
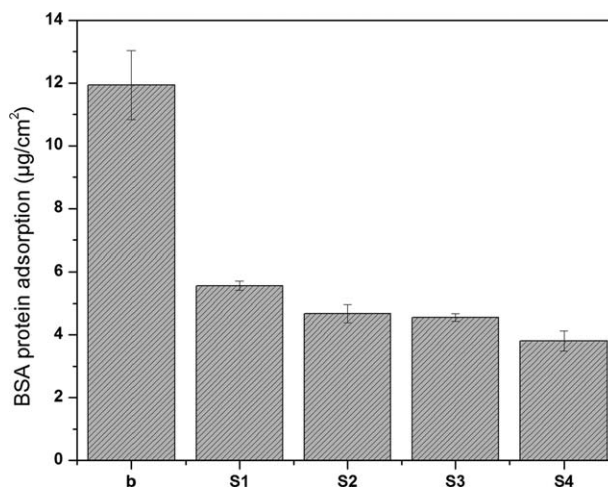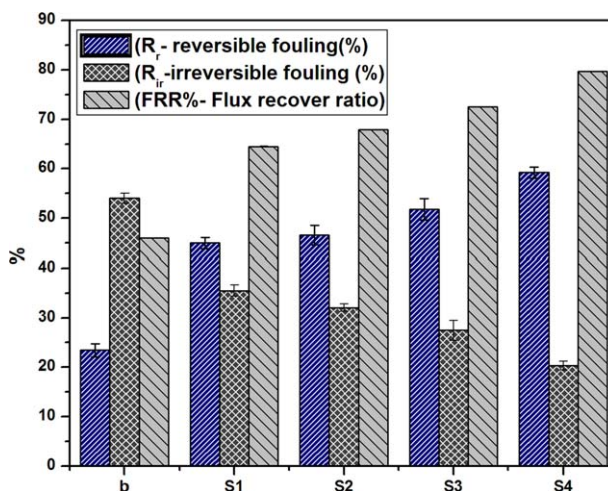

Figure 9. Fouling analysis results of PPSU-SO$_3$H -PPSU membranes. [Color figure can be viewed in the online issue, which is available at wileyonlinelibrary.com.]

Table IV. Fouling Resistance Results of PPSU-SO₃H incorporated PPSU Membranes in Protein Filtration

Membrane	Membrane resistance $R_m \times 10^{11}$ (m^{-1})	Pore plugging resistance $R_p \times 10^{11}$ (m^{-1})	Cake layer resistance $R_c \times 10^{11}$ (m^{-1})	Total resistance $R_t \times 10^{11}$ (m^{-1})
b	1.20 (±0.01)	1.40 (±0.31)	3.35 (±0.42)	5.95 (±1.04)
S1	0.94 (±0.07)	0.51 (±0.12)	2.72 (±0.24)	4.18 (±0.61)
S2	0.84 (±0.02)	0.39 (±0.09)	2.71 (±0.32)	3.95 (±0.60)
S3	0.76 (±0.08)	0.28 (±0.22)	2.61 (±0.12)	3.6 (±0.50)
S4	0.64 (±0.17)	0.16 (±0.04)	2.32 (±0.26)	3.12 (±0.66)

adhesion for protein molecules, during operation. As a result, the membrane (S3 andS4) gives lower values of R_c (Cake layer resistance) and R_p (pore plugging resistance) than pure PPSU membrane (b) (given in Table IV).

Furthermore, after protein filtration, all membranes were washed with distilled water and subjected to pure water flux measurement to evaluate the reusability.[40] From the flux results, the FRR (Flux recovery ratio) was calculated to determine the flux recovery of the modified membranes and results obtained are shown in Figure 9. The more hydrophobic PPSU membrane provides lower FRR value of 45.9 (±0.11), due to the occurrences of irreversible fouling within the membrane pores. The modified membrane (S3 and S4) gives higher FRR value of 72.5 (±0.32) and 79.6 (±0.62), respectively, which means that more hydrophilic membrane surfaces avoid the irreversible pore plugging, during BSA filtration process. Moreover, the previous results of the contact angle also support these antifouling results.

CONCLUSION

In this article, all PPSU-SO₃H entangled PPSU membranes were prepared via phase inversion method. The significant impact of adding PPSU-SO₃H was shown by enhancing the membrane surface properties. The conclusions are mentioned as follows:

1. The morphological results (SEM) proved that increasing the amount of PPSU-SO₃H has shown improvement in the finger like pore growth (sub layer) and high porous membrane surface. The resulted membranes shows inter connected membrane morphology.
2. XRD and mechanical strength analysis revealed the presence of incompatibility interaction during PPSU-SO₃H entanglement in the PPSU matrix. Especially, addition of 15–25 wt % of PPSU-SO₃H results the loosely packed membrane structure, which was the main factor in increasing the mean pore size of the membrane. The resultant membrane (S4) showed poor BSA rejection than that of membrane (S3).
3. The major results such as contact angle, flux of modified membranes showed great hydrophilic characteristics by adding PPSU-SO₃H to hold the hydration layer on the membrane surface (S1–S4). At the same time, the improved antifouling a phenomenon of all modified membranes was confirmed through the major results such BSA adsorption, FRR (%), and resistance in series model. Finally, the membrane (S3) shows potential antifouling surface properties with better BSA protein rejection. Therefore, these modified

membranes will have a great impact on separation and purification of protein bio molecules and drugs. The future work will be carried out on macromolecular PPSU-SO₃H chains to anchor the nanoparticles to produce different potential surfaces. Therefore, these nano MgO anchored membranes will have good impact in the field of biotechnology and bacterial consortium application.

REFERENCES

1. Liu,T. Y.; Zhang, R. X.; Li, Q.; Van der Bruggen, B.; Wang, X.-L. *J. Membr. Sci.* **2014**, *472*, 119.
2. Kumar, M.; Ulbricht, M. *Polymer* **2014**, *55*, 354.
3. Kumar, M.; Ulbricht, M. *Sep. Purif. Technol.* **2014**, *127*, 181.
4. Guan, R.; Zou, H.; Lu, D.; Gong, C.; Liu, Y. *Eur. Polym. J.* **2005**, *41*, 1554.
5. Liu, Y.; Yue, X.; Zhang, S.; Ren, J.; Yang, L.; Wang, Q. *Sep. Purif. Technol.* **2012**, *98*, 298.
6. Luo, J.; Meyer, A. S.; Jonsson, G.; Pinelo, M. *Biochem. Eng. J.* **2014**, *83*, 79.
7. Moghimifar, V.; Raisi, A.; Aroujalian, A. *J. Membr. Sci.* **2014**, *461*, 69.
8. Fan, X.; Su, Y.; Zhao, X.; Li, Y.; Zhang, R.; Zhao, J. *J. Membr. Sci.* **2014**, *464*, 100.
9. Kerres, J. A. *Fuel Cells.* **2005**, *5*, 230.
10. Van der Bruggen, B. *J. Appl. Polym. Sci.* **2009**, *114*, 630.
11. Cheng, Q.; Cui, Z.; Li, J.; Qin, S.; Yan, F.; Li, J. *J. Power Sources.* **2014**, *266*,401.
12. Jung, M. S.; Kim, T. H.; Yoon, Y. J.; Kang, C. G.; Yu, D. M.; Lee, J. Y. *J. Membr. Sci.* **2014**, *459*, 72.
13. Li, Y.; Zhang, H.; Li, X.; Zhang, H.; Wei, W. *J. Power Sources* **2013**, *233*, 202.
14. Guan, R.; Zou, H.; Lu, D.; Gong, C.; Liu, Y. *Eur. Polym. J.* **2005**, *41*,1554.
15. Malaisamy, R.; Mohan, D.; Rajendran, M. *J. Colloid Interface Sci.* **2002**, *254*, 129.
16. Huang, J.; Zhang, K.; Wang, K.; Xie, Z.; Ladewig, B.; Wang, H. *J. Membr. Sci.* **2012**, *423*, 362.
17. Kumar, R.; Isloor, A. M.; Ismail, A. F.; Matsuura, T. *J. Membr. Sci.* **2013**, *440*, 140.
18. Dulebohn, J.; Ahmadiannamini, P.; Wang, T.; Kim, S.; Pinnavaia, T. J.; Tarabara, V. V. *J. Membr. Sci.* **2014**, *453*, 478.

19. Jayalakshmi, A.; Rajesh, S.; Senthilkumar, S.; Mohan, D. *Sep. Purif. Technol.* **2012**, *90*, 120.

20. Li, Q.; Bi, Q.; Lin, H. H.; Bian, L. X.; Wang, X. L. *J. Membr. Sci.* **2013**, *427*, 155.

21. Jamshidi Gohari, R.; Halakoo, E.; Nazri, N. A. M.; Lau, W. J.; Matsuura, T.; Ismail, A. F. *Desalination* **2014**, *335*, 87.

22. Eren, E.; Sarihan, A.; Eren, B.; Gumus, H.; Kocak, F. O. *J. Membr. Sci.* **2015**, *475*, 1.

23. Yu, L. Y.; Xu, Z. L.; Shen, H. M.; Yang, H. *J. Membr. Sci.* **2009**, *337*, 257.

24. Yu, L.; Zhang, Y.; Zhang, B.; Liu, J.; Zhang, H.; Song, C. *J. Membr. Sci.* **2013**, *447*, 452.

25. Chiang, Y. C.; Chang, Y.; Higuchi, A.; Chen, W. Y.; Ruaan, R. C. *J. Membr. Sci.* **2009**, *339*, 151.

26. Rajesh, S.; Ismail, A. F.; Mohan, D. *RSC Adv.* **2012**, *2*, 6854.

27. Zhang, Y.; Zhao, J.; Chu, H.; Zhou, X.; Wei, Y. *Desalination* **2014**, *344*, 71.

28. Chang, I. S.; Kim, S. N. *Process Biochem.* **2005**, *40*, 1307.

29. Klaysom, C.; Ladewig, B. P.; Lu, G. Q. M.; Wang, L. *J. Membr. Sci.* **2011**, *368*, 48.

30. Rahimpour, A.; Madaeni, S. S.; Ghorbani, S.; Shockravi, A.; Mansourpanah, Y.; *Appl. Surf. Sci.* **2010**, *256*, 1825.

31. Hwang, L. L.; Tseng, H. H.; Chen, J. C. *J. Membr. Sci.* **2011**, *384*, 72.

32. Tsai, H.; Huang, D.; Ruaan, R.; Lai, J. *Ind. Eng. Chem. Res.* **2001**, *40*, 5917.

33. Ma, X.; Su, Y.; Sun, Q.; Wang, Y.; Jiang, Z. *J. Membr. Sci.* **2007**, *292*, 116.

34. Fan, X.; Su, Y.; Zhao, X.; Li, Y.; Zhang, R.; Zhao, J. *J. Membr. Sci.* **2014**, *464*, 100.

35. Arthanareeswaran, G.; Thanikaivelan, P.; Raajenthiren, M. *Mater. Sci. Eng. C* **2009**, *29*, 246.

36. Hwang, L. L.; Tseng, H. H.; Chen, J. C. *J. Membr. Sci.* **2011**, *384*, 72.

37. Zhou, J.; Meng, S.; Guo, Z.; Du, Q.; Zhong, W. *J. Membr. Sci.* **2007**, *305*, 279.

38. Sun, J.; Wu, L. *Colloids Surf. B: Biointerfaces.* **2014**, *123C*, 33.

39. Arthanareeswaran, G.; Mohan, D.; Raajenthiren, M. *Appl. Surf. Sci.* **2007**, *253*, 8705.

40. Jayalakshmi, A.; Rajesh, S.; Kim, I. C.; Senthilkumar, S.; Mohan, D.; Kwon, Y. N. *J. Membr. Sci.* **2014**, *465*, 117.